

# Neutron to proton ratios of quasiprojectile and midrapidity emission in the $^{64}\text{Zn} + ^{64}\text{Zn}$ reaction at 45 MeV/nucleon

D. Thériault <sup>\*</sup>,<sup>1</sup> J. Gauthier,<sup>1</sup> F. Grenier,<sup>1</sup> F. Moisan,<sup>1</sup> C. St-Pierre,<sup>1</sup> R. Roy,<sup>1</sup> B. Davin,<sup>2</sup> S. Hudan,<sup>2</sup> T. Padaszynski,<sup>2</sup> R.T. de Souza,<sup>2</sup> E. Bell,<sup>3</sup> J. Garey,<sup>3</sup> J. Iglío,<sup>3</sup> A.L. Keksis,<sup>3</sup> S. Parketon,<sup>3</sup> C. Richers,<sup>3</sup> D.V. Shetty,<sup>3</sup> S.N. Soisson,<sup>3</sup> G.A. Souliotis,<sup>3</sup> B.C. Stein,<sup>3</sup> and S.J. Yennello<sup>3</sup>

<sup>1</sup>*Laboratoire de Physique Nucléaire, Département de Physique, Université Laval, Québec, Canada G1K 7P4.*

<sup>2</sup>*Department of Chemistry and Indiana University Cyclotron Facility, Indiana University, Bloomington, IN 47405, USA*

<sup>3</sup>*Cyclotron Institute Texas A&M University, College Station, TX 77843, USA*

(Dated: August 15, 2018)

Simultaneous measurement of both neutrons and charged particles emitted in the reaction  $^{64}\text{Zn} + ^{64}\text{Zn}$  at 45 MeV/nucleon allows comparison of the neutron to proton ratio at midrapidity with that at projectile rapidity. The evolution of N/Z in both rapidity regimes with increasing centrality is examined. For the completely re-constructed midrapidity material one finds that the neutron-to-proton ratio is above that of the overall  $^{64}\text{Zn} + ^{64}\text{Zn}$  system. In contrast, the re-constructed ratio for the quasiprojectile is below that of the overall system. This difference provides the most complete evidence to date of neutron enrichment of midrapidity nuclear matter at the expense of the quasiprojectile.

PACS numbers: 25.70.Lm, 25.70.Mn

The density dependence of the asymmetry term for nuclear matter is a topic of considerable interest [1, 2]. Based on thermodynamic considerations it is possible for the binary nuclear fluid to fractionate into a proton-rich high density phase and a neutron-rich low density phase [1]. A manifestation of the density dependence of the asymmetry term from a kinetic perspective would involve the preferential transport of neutrons as compared to protons (“isospin diffusion”) when two heavy nuclei collide [3, 4, 5]. The overlapping tails of the two colliding nuclei leads to a low-density region into which the preferential flux of neutrons may occur. Neutron enrichment of the low density phase at midrapidity in comparison to the high density phase at the projectile and target rapidity might be a result of the density dependence of the asymmetry term. Following the contact phase of the collision, larger surface-to-volume ratio for transiently deformed reaction partners may also result in the preferential emission of neutron-rich clusters in the direction of the contact [6, 7]. Experimental results [8, 9, 10, 11, 12, 13] show that light particles and fragments emitted at midrapidity exhibit a neutron enrichment compared to the quasiprojectile (QP) or quasi-target (QT) in mid-peripheral collisions. Results with free-neutron detection aiming to reconstruct completely the midrapidity material (MRM) [14] have been obtained in the reaction  $^{129}\text{Xe} + ^{nat}\text{Sn}$  at 40 MeV/nucleon. The conclusions of the authors were that, on average, the MRM and the bulk system have an indistinguishable value of their N/Z ratios [14]. In a recent analysis, also with free-neutron detection, results obtained for the  $^{58}\text{Ni} + ^{58}\text{Ni}$  at 52 MeV/nucleon [15]

show that the N/Z ratio of the QP is below the ratio of the initial system and that the MRM ratio could be above the ratio of the initial system. Both experiments used different experimental setups to match neutron and charged particle data. In the present article, we report on an experimental evaluation of the MRM and QP N/Z ratios made using a single setup which should allow a more precise measurement of the N/Z ratios.

To examine the potential neutron enrichment of midrapidity nuclear matter we elected to study a symmetric projectile-target system thus eliminating any initial driving force towards N/Z equilibration. The experiment was performed at the Cyclotron Institute of Texas A&M University where a  $^{64}\text{Zn}$  beam, accelerated to 45 MeV/nucleon, bombarded a self-supporting 5 mg/cm<sup>2</sup>  $^{64}\text{Zn}$  target. Charged reaction products were detected with the FIRST array, consisting of three annular telescopes denoted T1 (270 $\mu\text{m}$  Si(IP)-1mm Si(IP)-CsI(Tl)/PD), T2 (300 $\mu\text{m}$  Si(IP)-CsI(Tl)/PD), and T3 (300 $\mu\text{m}$  Si(IP)-CsI(Tl)/PD). These telescopes subtended angles from 2.07° to 27.48° in the laboratory. Isotopic resolution was achieved for ions up to Z=12 in T1, Z=8 in T2, and Z=7 in T3 [16]. Charged particles emitted at larger angles ( $36.38^\circ \leq \theta_{lab} < 51.11^\circ$ ) were detected by LASSA telescopes which provided isotopic resolution for Z $\leq$ 6 [17]. Charge identification starts at Z=3 for T1, Z=2 for T2 and Z=1 for T3. The electronic trigger required the detection of at least one particle in FIRST. To detect emitted neutrons, 7 Bicron BC-501A liquid scintillator cells readout by photomultiplier tubes were mounted outside the scattering chamber at polar angles of 27°, 35°, 50°, 63°, 75°, 105°, 145°. Neutron energies were determined by time-of-flight measurements and spectra were corrected for background emission using a shadow bar technique. Energetic protons at forward angles were rejected using thin scintillator

<sup>\*</sup>Correspondence to D. Thériault, email: dany.theriault.1@ulaval.ca

paddles placed directly in front of the neutron detectors. The neutron efficiency of the experimental setup was determined by using GEANT4 [18] simulations.

We focus on peripheral and mid-peripheral collisions in which a fragment with  $Z \geq 9$  and a parallel velocity (beam direction) larger than the center of mass velocity (4.5 cm/ns) was detected. The most likely origin of this large atomic number,  $Z_{res}$ , high-velocity fragment is the decay residue of the QP following a non-central collision. Due to the experimental acceptance the corresponding residue of the QT is not detected. Nevertheless, due to the symmetry of the system the average properties of the QP and the QT are inferred to be the same. In addition, a multiplicity of 4 charged particles and a total detected charge of 25 or more,  $Z_{tot} \geq 25$  ( $Z_{BEAM}=30$ ), were also required to ensure sufficient reconstruction of the QP. Non-isotopically resolved ions in FIRST were assigned an average mass based on the initial N/Z of the system for  $Z \geq 29$  or on the evaporation attractor line [19].

To compare the N/Z of the QP to that of the MRM we reconstructed the QP based on the measured residue, bound clusters ( $A \geq 2$ ), and free nucleons. For bound clusters, the QP source reconstruction procedure relies on three hypotheses [20]: 1) the heaviest fragment selected as the QP evaporation residue has a velocity close to the QP velocity, 2) the QP emission is isotropic in its reference frame and 3) all the particles with a parallel velocity greater than that of the residue (forward distribution) were emitted from the QP.

Clusters with a minimum parallel velocity (to minimize the contribution originating from the QT) are attributed to the QP or MRM based on their relative velocity with the QP. For each cluster-QP residue pair, the norm of the relative velocity between a cluster and the residue,  $V_{rel}$ , is calculated. The resulting spectra of  $V_{rel}$  for hydrogen and helium isotopes with  $Z_{res} = 14$  and  $Z_{res} = 21$  are displayed in Fig. 1. Evident from these spectra is the fact that backward emission ( $V_{rel} < 0$ ) is favored over forward emission ( $V_{rel} > 0$ ). This result is consistent with previous work [8, 21, 22]. To facilitate this comparison the distribution for  $V_{rel} > 0$  has been reflected, consistent with the isotropic decay hypothesis of the QP. A striking feature of these spectra is that the enhancement of yield for  $V_{rel} < 0$  is particularly evident for neutron rich clusters such as  ${}^6\text{He}$  as compared to  ${}^3\text{He}$  [9, 10]. Deuterons and tritons also exhibit a strong preference for the backward direction. Based upon such experimental  $V_{rel}$  spectra, probability tables for attributing a cluster to the QP are constructed. For particles emitted forward of the QP residue the attribution probability is taken to be unity while the probability for backward emitted particles (parallel velocity less than that of the QP residue) the attribution probability is obtained by dividing the forward  $V_{rel}$  distribution by the backward distribution. The attribution probability, for each cluster, obtained in this manner depends on both  $V_{rel}$  and  $Z_{res}$  and is

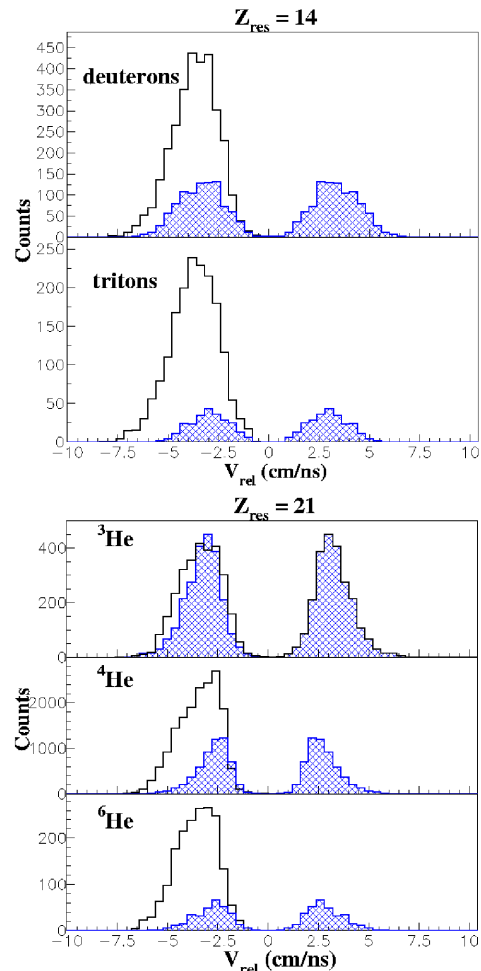


FIG. 1: (Color online) Total relative velocity between a cluster and the QP residue,  $V_{rel}$ , backward distribution (clear) and forward  $V_{rel}$  distribution backward-reflected (shadowed) for  $Z=1$  isotopes coupled with a QP residue of  $Z=14$  (upper panel) and for  $Z=2$  isotopes coupled with a QP residue of  $Z=21$  (lower panel).

applied on an event-by-event basis. This approach to re-construct the QP has been previously applied to simulations of the collision (DIT+GEMINI [23, 24]) and has been shown to correctly attribute more than 85% of the particles emitted in mid-peripheral and peripheral collisions [20]. Further details about the reconstruction method and its efficiency are given in Ref. [20, 25, 26, 27]. Backward emitted particles that were not assigned to the QP belong to the MRM if their parallel velocity is greater than 2 cm/ns in the reference frame of the QT, which is moving at velocities determined in the proton multisource analysis.

In order to attribute protons and neutrons to the QP and MRM, the average proton and neutron multiplicities were extracted for three classes of events namely  $Z_{res} = 9 - 13$ ,  $14 - 18$  and  $19 - 26$ . It has been previously

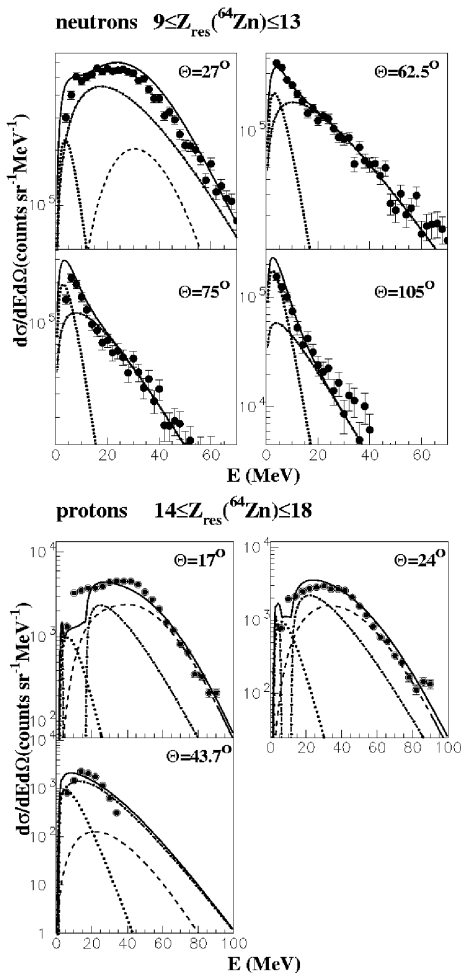


FIG. 2: Multisource fit for free neutrons (upper panel) and free protons (lower panel) at selected angles. Selected centrality classes defined with the charge of the QP residue are shown. QP (dashed lines), QT (dotted lines), MRM (dotted-dashed lines) and total (full lines) contributions are illustrated.

shown that  $Z_{res}$  is correlated to the excitation energy per nucleon of the QP and is thus a reasonable measure of the centrality of the collision [28, 29]. Proton multiplicities are obtained *via* a moving source analysis of energy spectra at  $\theta_{lab}=17^\circ$ ,  $24^\circ$ , and  $43.7^\circ$  while neutron multiplicities were extracted from a moving source analysis of the background and efficiency corrected energy spectra at 7 angles. Energy spectra at all angles are fitted simultaneously with the emission from three sources, QP, QT and a midrapidity “source”, although the neutron spectra and proton spectra are treated independently. The midrapidity source, though perhaps not a single physical statistical source, is necessary to describe the dynamical nucleon emission at midrapidity that contributes to the N/Z of the MRM. Each source is characterized by a temperature parameter  $T$ , velocity  $V_s$ , Coulomb barrier  $B_c$  (protons) and a normalization factor  $N$ , related to its multiplicity. The nucleon energy ( $E$ ) distributions are

fitted under the assumption of surface emission for the QT and QP sources and volume emission for the MRM by [28, 29, 30, 31, 32]:

$$\left(\frac{d^2\sigma}{d\Omega dE}\right) = \frac{N}{kT^i} (E - B_c)^j \exp[-(E - B_c)/T] \quad (1)$$

where  $(i,j,k)=(2,1,4\pi)$  in the case of surface emission and  $(i,j,k)=(3/2,1/2,2\pi^{3/2})$  in the case of volume emission. Based on the symmetry of the system, it is assumed that QP and QT have the same multiplicity, temperature, and Coulomb barrier while the velocity of the MRM is fixed at the nucleon-nucleon center of mass velocity (4.5 cm/ns). The spectra associated with the three sources is transformed to the laboratory frame. Fig. 2 presents the results of the multisource fits for protons and neutrons at selected centrality classes and angles. As can be seen in these representative spectra the multi-source fits provide a reasonably good description of the measured energy spectra. The somewhat poor description of the high energy tail for the proton spectra at  $\theta_{lab}=43.7^\circ$  is due to a decreased triggering efficiency for fast protons in the LASSA telescopes. However, the uncertainty associated with the limited experimental data does not significantly effect the multiplicity associated with the QP and MRM. The parameters extracted from the multisource fits are presented in Table 1.

In Fig. 3, the dependence of the extracted proton and neutron average multiplicities on the quantity  $(Z_{proj} - Z_{res})$  is shown. This difference in atomic number is used as a measure of the centrality of the collision, with increasing  $(Z_{proj} - Z_{res})$  associated with increasing centrality. Evident in Fig. 3 is the slight increase (decrease) of the proton multiplicity for the MRM (QP) with increasing centrality. Measured MRM proton multiplicities are between 1.47 and 1.96 protons/event while QP proton multiplicities range from 1.51 to 0.93 protons/event. QP neutron multiplicities are between 0.81 and 0.95 neutron/event and are nearly equal to QP proton multiplicities for the most central collisions studied, a result consistent with the statistical decay of a nearly  $N=Z$  QP at high excitation. In contrast, the MRM neutron multiplicity increases from 2.22 to 3.25 neutrons/event with increasing centrality and is larger than MRM proton multiplicity. The QP is significantly larger in size (see Fig. 4) and presumably at near saturation density. Coulomb barrier suppresses QP statistical proton emission as compared to neutron emission from the QP. Nevertheless, the neutron multiplicity extracted for the MRM is two to three times larger than for the one associated with the QP. The extracted multiplicities were linearized as shown in Fig. 3 in order to provide a continuous relation between the multiplicities of free nucleons and centrality. Error bars extracted from the optimization are shown.

Evident in the top panel of Fig. 4 is the dependence of the atomic number of the reconstructed QP and MRM (free nucleons, particles and all heavier fragments) on centrality. With increasing centrality the size of the QP decreases from  $Z\approx 28$  to  $Z\approx 21$  while the size of the MRM

$Z_{res}$	$T_{MRM}$ (n/p)	$T_{QP}$ (n/p)	$V_{QP}$ (n/p)	$B_c$	$M_n$ (QP/MRM)	$M_p$ (QP/MRM)
9-13	10.9/7.7	2.7/4.3	8.1/7.8	0.06	0.95/3.25	0.93/1.73
14-18	10.7/6.8	2.0/3.7	8.4/8.1	0.38	0.84/2.95	1.01/1.96
19-26	10.5/6.5	2.2/2.7	8.4/8.4	1.00	0.81/2.22	1.51/1.47

TABLE I: Source parameters ( $T$ (MeV),  $V$ (cm/ns),  $B_c$ (MeV),  $M$ (nucleons/event)) extracted from the multi-source analysis

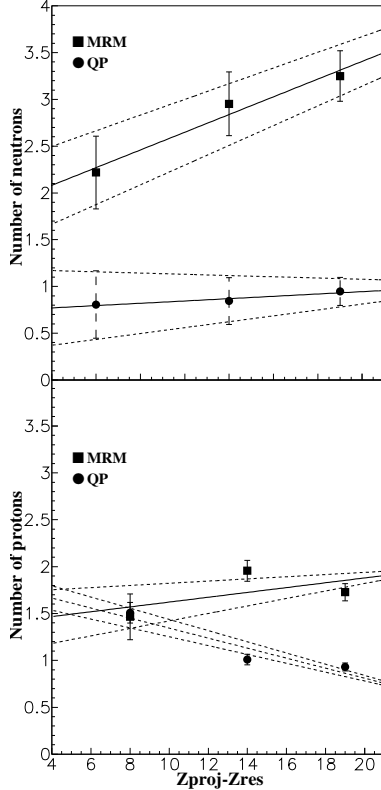


FIG. 3: Free neutron (upper panel) and proton (lower panel) average multiplicities as a function of the projectile charge minus the average QP residue charge. QP (dots) and MRM (squares) multiplicities are illustrated. Solid lines are fitted to the obtained values and dashed lines to the upper and lower uncertainties.

increases from a value of  $Z \approx 5$  to  $Z \approx 8$ . The decrease in the size of the QP is associated with an increase in the emitted charge. For peripheral collisions,  $Z_{res}=25$  and  $Z_{emitted}=3$  while for mid-peripheral collisions  $Z_{res}=9$  and  $Z_{emitted}=12$ , consistent with increased excitation. For the most central collisions presented, the atomic number of the QP and MRM are constant.

The average  $N/Z$  of the reconstructed QP and MRM (free nucleons, particles and all heavier fragments) are displayed in the lower panel of Fig. 4. A clustered charge of at least 2 units is required in the MRM to avoid MRM  $N/Z$  ratios computed only with free nucleons. The value of the  $N/Z$  ratio for the MRM (solid squares) increases with increasing centrality from 1.19 (peripheral) to 1.35 (semi-peripheral). For reference the  $N/Z$  of the

system (1.13) is indicated as the dashed line. Over the entire centrality range examined, the  $N/Z$  of the MRM exceeds the  $N/Z$  of the system. In contrast, the  $N/Z$  of the QP (solid circles) is relatively constant over the same centrality range with a value of  $\approx 1.07 \pm 0.04$ , slightly less than the  $N/Z$  ratio of the original system. The uncertainty in the reconstructed  $N/Z$  lies largely with the uncertainty in the nucleon emission. To assess this uncertainty we used extreme assumptions regarding the contribution of free nucleon emission to the  $N/Z$  of the QP and MRM consistent with the measured multiplicities displayed in Fig. 3. The maximum (minimum) neutron multiplicity possible for a particular centrality was assumed to be associated with the minimum (maximum) proton multiplicity resulting in the largest (smallest)  $N/Z$ . The uncertainties displayed therefore correspond to the maximum uncertainties on the  $N/Z$  due to the free nucleon multiplicities. Despite the large uncertainties associated with the  $N/Z$  for the MRM, for mid-peripheral collisions, a clear neutron enrichment is observed at the expense of the QP. In addition to the uncertainty associated with the free nucleon multiplicities, tests were conducted to evaluate the uncertainty associated with the minimal clustered charge required in the MRM, the mass of the non-isotopically resolved fragments, and also the Coulomb influence of the target on the particles with differing  $N/Z$ . In all these tests, a neutron enrichment of the MRM is observed and the calculated MRM  $N/Z$  ratio is between 1.29 and 1.37 for the most central collisions studied here.

To understand the observed trends in  $N/Z$  for the QP and MRM, we have further examined the  $N/Z$  associated with clusters ( $A \geq 2$ ). In the case of the MRM (open squares), the  $N/Z$  is constant with centrality and has a value close to that of the  $N/Z$  of the system. In contrast, for the case of the QP (open circles), where we additionally exclude the QP residue from the calculation of the  $N/Z$ , a centrality dependence is observed. While for the most peripheral collisions, the  $N/Z$  of the clusters attributed to the QP is approximately 0.9, with increasing centrality this value increases towards 1.05. These observed trends in  $N/Z$  associated with clusters can be understood quite simply. In the case of the MRM, the tendency to clusterize at low density is strongly driven by the alpha particle formation and to a lesser extent deuteron formation. Formation of these  $N=Z$  clusters dominates all other clusters. Formation of other neutron-rich clusters, such as tritons and  ${}^6\text{He}$ , explains why the average value of  $N/Z$  is larger than unity. Examples of the relative yield of these light clusters is apparent in Fig. 1. In the case of the QP, the measured  $N/Z$  associ-

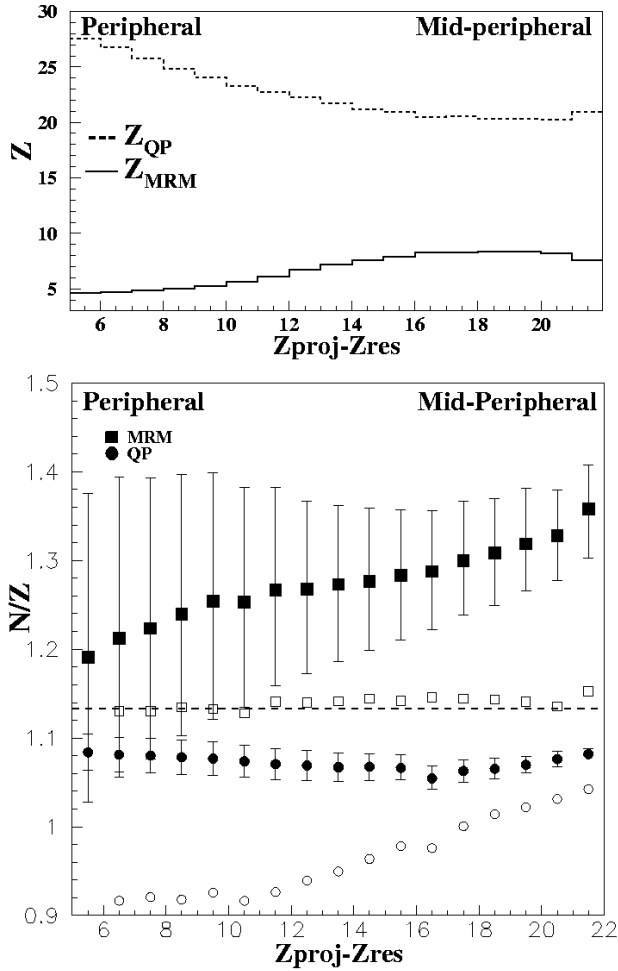


FIG. 4: Upper panel: Average charge of the QP and MRM as a function of the charge difference between the projectile and the residue. Lower panel: Average N/Z ratios of QP (solid circles) and MRM (solid squares) as a function of the charge difference between the projectile and the residue. The open symbols correspond to the clusters. Thin dotted line: original N/Z of the projectile and target. Errors due to multisource fit uncertainty for free nucleons are reported.

ated with clusters is primarily driven by the ratio of  ${}^3\text{He}$  and  ${}^4\text{He}$  at low excitation and the emission of heavier neutron-rich clusters with increasing excitation.

Consequently, the increase in the N/Z for the MRM stems largely from the preferential free neutrons as compared to free protons and clusters in this regime. One can therefore conclude from Fig. 4 that, on average, the QP, and presumably the QT, preferentially transfer a few neutrons to the MRM. While the small number of neutrons transferred does not change the QP N/Z significantly because of its large size ( $21 \leq \langle Z_{QP} \rangle \leq 28$ ), it is a significant change for the much smaller MRM ( $5 \leq \langle Z_{MRM} \rangle \leq 8$ ). For the presently studied symmetric system, the Coulomb push of emitted particles by the QP and QT should be roughly equal at midrapidity thus contributing negligibly to a systematic suppression of neutron-rich clusters in the MRM. Neutron skin effects, for elements of the size of the  ${}^{64}\text{Zn}$ , should also be negligible [33].

In summary, we observed that the average N/Z ratio of MRM is above the N/Z ratio of the original system for mid-peripheral reactions of the  ${}^{64}\text{Zn}+{}^{64}\text{Zn}$  system at 45 MeV/nucleon. This neutron enrichment of midrapidity nuclear material is at the expense of the QP that systematically has a N/Z ratio below that of the system. A likely origin for the preferential transfer of neutrons towards midrapidity is a density dependence of the symmetry energy [34, 35].

#### Acknowledgments

This work was supported in part by the Natural Sciences and Engineering Research Council of Canada, the Fonds pour la Formation de Chercheurs et l'Aide à la Recherche du Québec, the U.S. Department of Energy through Grants No. DE-FG-92ER40714 (IU), DE-FG03-93ER40773 (TAMU) and the Robert A. Welch Foundation through Grant No. A-1266.

- 
- [1] H. Müller and B.D. Serot. *Phys. Rev. C* **52**, 2072(1995).
  - [2] W. Udo Schröder B. Li. *Isospin Physics in Heavy-Ion Collisions at Intermediate Energies*, Nova Science Publishers, Inc., 2001.
  - [3] L. Shi and P. Danielewicz. *Phys. Rev. C* **68**, 064604 (2003).
  - [4] Bao-An Li. *Phys. Rev. C* **69**, 034614 (2004).
  - [5] V. Baran et al. *Phys. Rev. C* **72**, 064620 (2005).
  - [6] S. Hudan et al. *Phys. Rev. C* **70**, 031601 (2004).
  - [7] S. Hudan et al. *Phys. Rev. C*, (in press).
  - [8] E. Plagnol et al. *Phys. Rev. C* **61**, 014606(1999).
  - [9] J.F. Dempsey et al. *Phys. Rev. C* **54**, 1710(1996).
  - [10] S. Hudan et al. *Phys. Rev. C* **71**, 054604 (2005).
  - [11] Y. Larochelle et al. *Phys. Rev. C* **62**, 051602(R)(2000).
  - [12] P.M. Milazzo et al. *Phys. Lett. B* **509**, 204(2001).
  - [13] D. Shetty et al. *Phys. Rev. C* **68**, 054605 (2003).
  - [14] L.G. Sobotka et al. *Phys. Rev. C* **62**, 031603(R)(2000).
  - [15] D. Thériault et al. *Phys. Rev. C* **71**, 014610 (2005).
  - [16] T. Padaszynski et al. *Nucl. Inst. and Meth. A* **547**, 464 (2005).
  - [17] B. Davin et al. *Nucl. Inst. and Meth. A* **473**, 302(2001).
  - [18] S. Agostinelli et al. *Nucl. Inst. and Meth. A* **506**, 250 (2003).
  - [19] R. J. Charity. *Phys. Rev. C* **58**, 1073(1998).
  - [20] L. Gingras et al. *XXXVI international winter meeting on nuclear physics, Bormio (Italy)*, 265 (1998).
  - [21] C.P. Montoya et al. *Phys. Rev. Lett.* **73**, 3070(1994).
  - [22] T. Lefort et al. *Nucl. Phys. A* **662**, 397(2000).
  - [23] R.J. Charity et al. *Nucl. Phys. A* **483**, 371(1988).
  - [24] L. Tassan-Got and C. Stéphan. *Nucl. Phys. A* **524**,

121(1991).

- [25] Z. He et al. *Phys. Rev. C* **63**, 011601(2000).
- [26] L. Gingras et al. *Phys. Rev. C* **65**, 061604(2002).
- [27] Z. He et al. *Phys. Rev. C* **65**, 014606(2002).
- [28] D. Doré. *Phys. Lett. B* **491**, 15(2000).
- [29] G. Lanzano et al. *Nucl. Phys. A* **683**, 566(2001).
- [30] A.S. Goldhaber. *Phys. Rev. C* **17**, 2243(1978).
- [31] R. Wada et al. *Phys. Rev. C* **39**, 497(1989).
- [32] Y. Larochelle et al. *Phys. Rev. C* **59**, 565(1999).
- [33] L.G. Sobotka. *Acta Physica Polonica B* **31**, 1535 (2000).
- [34] V. Baran et al. *Nucl. Phys. A* **632**, 287(1998).
- [35] Y. Zhang et al. *Phys. Rev. C* **71**, 024604 (2005).